



Germacranolides from *Artemisia myriantha* and their conformation

Ho-Fai Wong, Geoffrey D. Brown*

Department of Chemistry, The University of Hong Kong, Pokfulam Road, Hong Kong

Received in revised form 19 November 2001

Abstract

The CH_2Cl_2 extract of the aerial parts of *Artemisia myriantha* afforded three germacranolides derived from 13-acetoxy-3 β -hydroxy-germacra-1(10)*E*,4*E*,7(11)-trien-12,6 α -olide, whose structures were elucidated by 2D-NMR spectroscopic analyses. Some conclusions are drawn about the possible conformations of the ten-membered germacranolide ring system from the exchange peaks seen in the NOESY spectra, and an estimate is made of the energy barrier to ring-flipping from variable-temperature NOESY experiments. The conclusions reached were supported by molecular modeling studies and an NMR spectroscopic investigation of the commercially available germacranolide, parthenolide. © 2002 Elsevier Science Ltd. All rights reserved.

Keywords: *Artemisia myriantha* Wall. ex. Bess.; Compositae; Germacranolide sesquiterpenes; 13-Acetoxy-3 β -hydroxy-germacra-1(10)*E*,4*E*,7(11)-trien-12,6 α -olide; Tigloyl ester; Propanoyl ester; 3-Methylbutanoyl ester; Parthenolide; 2D-NMR; Variable temperature-EXSY; Molecular modeling; Conformational analysis

1. Introduction

Artemisia myriantha Wall. ex Bess. (Compositae) is used in traditional Chinese medicine for treating menorrhagia and inflammatory diseases (Ling, 1986). A previous communication concerning the phytochemistry of this species described the guaianolide, arglabin (Appendino et al., 1991), which is currently employed for treating certain types of cancer in the former USSR (Adekenov, 2000a) and is also under clinical investigation in the USA (Adekenov, 2000b), as the major constituent.

2. Results and discussion

The CH_2Cl_2 extract of the aerial parts of *A. myriantha* yielded, in addition to the known compound arglabin (Appendino et al., 1991), compounds **1–4** after separation by CC and HPLC. The structure of 13-acetoxy-3 β -hydroxy-germacra-1(10)*E*,4*E*,7(11)-trien-12,6 α -olide (**1**) (Fig. 1), previously isolated from a *Pentzia* species (Zdero and Bohlmann, 1990), was elucidated by 2D-NMR spectroscopic analysis and by comparison of its ^1H spectrum with that reported in the literature. Fully assigned ^{13}C NMR spectral data for **1** are now reported in Table 1

for the first time. To the best of our knowledge, only the 3-acetate derivative of **1** was described previously (Jakupovic et al., 1988, 1991); in both citations this compound was isolated from an *Artemisia* species.

Compound **2** was identified as the 3 β -tigloyl ester of **1** by HREIMS (388.1885 for $\text{C}_{22}\text{H}_{28}\text{O}_6$) and 2D-NMR spectroscopic analysis (Tables 1 and 2, Fig. 2) which resulted in unambiguous assignments for all of the ^{13}C and ^1H nuclei in the molecule. The 3 β -propanoyl ester (**3**) (362.1728 for $\text{C}_{20}\text{H}_{26}\text{O}_6$) and the 3 β -(3-methylbutanoyl) ester (**4**) (390.2040 for $\text{C}_{22}\text{H}_{30}\text{O}_6$) of **1** gave essentially the same 2D-NMR spectral correlations as those found in **2** for the germacranolide portion of the molecule (Fig. 2) and rigorous assignment of all of the NMR resonances for these natural products are also reported in Tables 1 and 2.

Knowledge of the ^1H assignments was particularly useful in interpreting the NOESY spectra of **1–4**, in which the absence of a nuclear Overhauser enhancement (NOE) between H-3 and H-6 was consistent with a *trans* relative stereochemistry between the 3-hydroxyl group and the 6-lactone oxygen, while the absence of nOe's between H-1/H-14 and H-5/H-15 indicated an *E* stereochemistry for the $\Delta^{1,10}$ and $\Delta^{4,5}$ double bonds. The absolute stereochemistry for compounds **1–4** is assumed to be the same as that previously reported for 3 β ,13-diacetoxy-germacra-1(10)*E*,4*E*,7(11)-trien-12,6 α -olide (artemisia glaucolide) isolated from other *Artemisia* species (Jakupovic et al., 1988).

* Corresponding author. Tel.: +852-2859-7915; fax: +852-2857-1586.

E-mail address: gdbrown@hkucc.hku.hk (G.D. Brown).

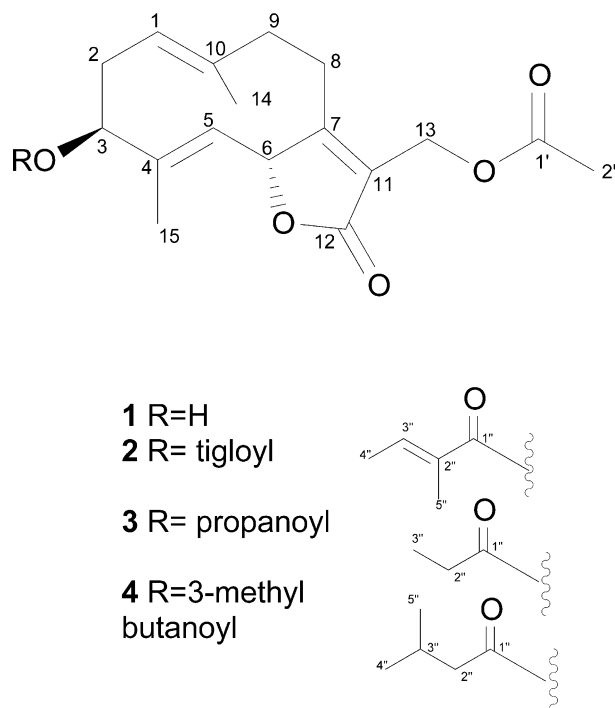


Fig. 1. Germacranolide sesquiterpenes isolated from *Artemisia myriantha*.

Interpretation of the correlations seen in the NOESY spectra for compounds **1–4** was made difficult by the presence of a large number of positive cross-peaks which were present, in addition to the negative cross-peaks that are normally associated with nuclear Overhauser enhancements between protons which can be used to assign relative stereochemistry and conformation (Fig. 3). Such positive cross-peaks are generally considered to be indicative of rapid chemical exchange on the NMR time-scale and are referred to as “EXSY-type” peaks in recognition of their origin (Braun et al., 1996). Since these positive peaks were largely associated with protons in the ten-membered ring of compounds **1–4**, rather than with the ring-substituents, it was considered that their occurrence indicated the possibility of conformational flexibility for the medium-sized germacrane ring-system at ambient temperature.

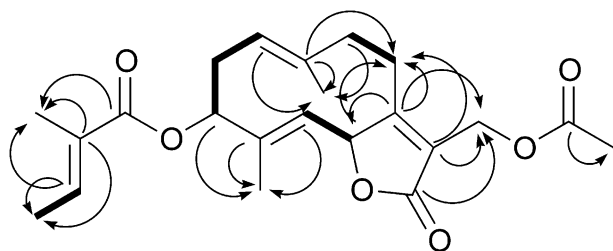


Fig. 2. HMBC and ^1H – ^1H COSY correlations used in establishing the planar structure of **2** (indicated by arrows from ^{13}C to ^1H and bold lines in the structure, respectively). Compounds **1**, **3** and **4** gave essentially the same correlations for the germacrane ring portion of the molecule.

Table 1
 ^{13}C NMR spectral assignments for compounds **1–5**

Position ^{a,b}	1	2	3	4	5
1 (CH)	126.4	125.5	125.4	125.4	125.3
2 (CH ₂)	34.4	31.4	31.4	31.4	24.1
3 (CH)	77.1	78.0	77.8	77.2	36.4
4 (C)	142.0	138.2	138.0	137.8	61.5
5 (CH)	120.6	122.1	122.2	122.2	66.4
6 (CH)	80.8	80.4	80.4	80.4	82.5
7 (C)	170.2	169.7	169.7	169.7	47.7
8 (CH ₂)	26.0	26.0	26.0	26.0	30.6
9 (CH ₂)	40.3	40.3	40.3	40.3	41.2
10 (C)	135.9	136.8	136.8	136.7	134.6
11 (C)	125.0	125.2	124.8	125.3	139.2
12 (C)	172.5	172.6	172.3	172.5	169.3
13 (CH ₂)	55.4	55.4	55.4	55.4	121.3
14 (CH ₃)	16.1	16.2	16.2	16.1	17.0
15 (CH ₃)	11.2	12.0	11.9	11.9	17.3
1' (C)	170.7	170.7	170.6	170.6	
2' (CH ₃)	20.8	20.8	20.9	20.8	
1''		166.9 (C)	173.4 (C)	172.5 (C)	
2''		128.1 (C)	27.8 (CH ₂)	43.5 (CH ₂)	
3''		137.7 (CH)	9.2 (CH ₃)	25.8 (CH)	
4''		14.4 (CH ₃)		22.4 (CH ₃) ^c	
5''		12.1 (CH ₃)		22.5 (CH ₃) ^c	

^a ^{13}C directly attached to ^1H determined by HSQC.

^b Multiplicity determined by DEPT indicated in parentheses.

^c Assignments interchangeable.

The hypothesis that the ten-membered ring in compound **1** was undergoing rapid flipping between two conformational states at the temperature of the NMR probehead (298 K) in CDCl_3 solution was confirmed in two ways. Firstly, the EXSY spectra of **1** was re-recorded at several different temperatures (268–308 K), and the ratio of the volume integrals for the EXSY cross-peaks for H-3, H-5 and H-9, relative to the volume integrals for the diagonal peaks associated with the two conformers for each of these protons (δ_{H} 4.26↔4.50; 4.38↔4.61; and 2.53↔2.67 ppm, respectively) were then used to calculate the rate of exchange (Perrin and Dwyer, 1990; Evans, 1995). This choice of temperatures was dictated by the need to record EXSY spectra under conditions associated with an exchange rate of 10^{-2} – 10^2 s^{-1} (Perrin and Dwyer, 1990),¹ while these three particular

¹ At exchange rates lower than 10^{-2} s^{-1} the off-diagonal peaks become very weak and it is difficult to obtain a reasonably good signal-to-noise ratio for accurate measurement of their volume integrals; whereas at rates above 10^2 s^{-1} more rapid exchange causes the cross-peaks to become broadened to the extent that they start to overlap with the diagonal peaks, making it difficult to measure the ratio of the two types of signal (which is needed to calculate the rate). Note that an alternative method for the determination of the rate of exchange from line-shape analysis of one-dimensional NMR spectra requires an estimation of the coalescence temperature, and typically works well for rates covering the range 1 – 10^4 s^{-1} (Perrin and Dwyer, 1990). The one-dimensional methodology would not be practical for studying exchange processes of **1** in CDCl_3 solution at 500 MHz, as the (extrapolated) coalescence temperature for many of the ^1H resonances in **1** are close to the boiling point of CDCl_3 .

Table 2
¹H NMR spectral assignments for compounds **1–5**

Position ^{a,b}	1	2	3	4	5
1	4.79 (<i>br</i>)	4.84 (<i>br</i>)	4.81 (<i>br</i>)	4.81(<i>br</i>)	5.22 (<i>br d</i> , 11.2)
2 α	2.45	2.56	2.52	2.52	2.19 (<i>d</i> , 14.3)
2 β	2.30	2.36	2.33	2.31	2.41
3 α	4.26 (<i>dd</i> , 10.0, 6.1)	5.23 (<i>dd</i> , 10.2, 6.2)	5.18 (<i>dd</i> , 10.3, 6.1)	5.20 (<i>dd</i> , 10.5, 6.2)	1.25 (<i>ddd</i> , 14.3, 13.3, 5.9)
3 β	—	—	—	—	2.15
5	4.38 (<i>d</i> , 10.1)	4.51 (<i>d</i> , 10.3)	4.49 (<i>d</i> , 10.2)	4.49 (<i>d</i> , 10.1)	2.79 (<i>d</i> , 9.4)
6	5.49 (<i>d</i> , 10.1)	5.47 (<i>d</i> , 10.3)	5.46 (<i>d</i> , 10.2)	5.46 (<i>d</i> , 10.1)	3.86 (<i>dd</i> , 9.4, 8.5)
7	—	—	—	—	2.79
8 α	3.00 (<i>dd</i> , 13.4, 8.2)	3.03 (<i>dd</i> , 12.5, 7.7)	3.02 (<i>dd</i> , 12.8, 7.5)	3.02 (<i>dd</i> , 13.5, 8.7)	2.16
8 β	2.24	2.27	2.24	2.24	1.71
9 α	2.17	2.22	2.22	2.21	2.18
9 β	2.53	2.54	2.55	2.53	2.37
13	4.85 (<i>br, d</i> , 12.8)	4.87 (<i>d</i> , 12.8)	4.86 (<i>d</i> , 12.6)	4.87 (<i>d</i> , 12.8)	6.32 (<i>d</i> , 3.5)
13	4.78 (<i>br, d</i> , 12.8)	4.80 (<i>d</i> , 12.8)	4.79 (<i>d</i> , 12.6)	4.80 (<i>d</i> , 12.8)	5.63 (<i>d</i> , 3.5)
14	1.60 (3H, <i>s</i>)	1.62 (3H, <i>s</i>)	1.61 (3H, <i>s</i>)	1.61 (3H, <i>s</i>)	1.71 (3H, <i>s</i>)
15	1.76 (3H, <i>s</i>)	1.76 (3H, <i>s</i>)	1.73 (3H, <i>s</i>)	1.74 (3H, <i>s</i>)	1.31 (3H, <i>s</i>)
2'	2.09 (3H, <i>s</i>)	2.09 (3H, <i>s</i>)	2.09 (3H, <i>s</i>)	2.09 (3H, <i>s</i>)	
2''	—	—	2.38 (2H, <i>q</i> , 7.5)	2.22 (2H)	
3''	—	6.91 (<i>q</i> , 7.1)	1.17 (3H, <i>t</i> , 7.5)	2.10	
4''	—	1.82 (3H, <i>d</i> , 7.1)	—	0.98 (3H, <i>d</i> , 6.9)	
5''	—	1.86 (3H, <i>s</i>)	—	0.98 (3H, <i>d</i> , 6.9)	

^a ¹H directly attached to ¹³C determined by HSQC.

^b Multiplicity and coupling constant(s) (in Hz), when resolved in 1-D NMR, indicated in parentheses.

protons were selected both because of a lack of interference from the other chemical shifts in the molecule when measuring diagonal and off-diagonal volume integrals and also because of their relative dispositions at well-spaced intervals around the germacrane ring. The results of variable temperature-EXSY experiments showed that the rates of exchange (k_{exch}) for all three protons at any given temperature were always very similar (Table 3); while Arrhenius plots (Atkins, 1999) of the logarithmic rate-dependence on the reciprocal of temperature confirmed that the activation barrier to the exchange process was also nearly identical for each of the three ring-protons under study ($E_a \approx 80$ – 85 kJ mol⁻¹; Fig. 4). These results were, therefore, entirely consistent with the postulated exchange process, which involves conformational changes for *all* of the protons in the ten-membered ring by a ring-inversion mechanism such as that shown in Fig. 5.

The second piece of evidence for a ring-flipping process being responsible for the exchange phenomenon observed in NMR spectroscopy, came from molecular modeling studies. Using the MM2 force field of the molecular simulation package MacroModel (Mohamadi et al., 1990), it was predicted that essentially only two possible conformations should exist for the ten-membered ring in compound **1** (ignoring trivial differences associated with the rotation of methyl groups which had little effect on the calculated energies of the two conformers). The energy gap between the lower energy conformer (A) and the higher energy conformer (B) was predicted to be less than 6 kJ mol⁻¹, and this

value was in good agreement with the results obtained from 1D ¹H NMR measurements of the relative populations ($[N]_A:[N]_B \approx 100:16$) of the two exchanging species at ambient temperature for the NMR probehead (298 K) from which an experimental energy difference of almost 5 kJ mol⁻¹ was calculated (see Experimental). It can be seen in Fig. 5 that the endocyclic tri-substituted double bonds are predicted to be nearly parallel in both conformers A and B, and that both bonds have been flipped by 180° in the higher energy conformer (B). The chemical shifts recorded for the alkene protons in the germacrane ring were relatively upfield (δ_H 4.38–5.31 ppm) for both ¹H partners participating in exchange and this would be consistent with the alkene protons of each one of the double bonds in the ring being located in the shielding region of the other double bond in both conformations, as seen in Fig. 5. The axial conformation of the bulky ring-hydroxyl group in

Table 3
 Rates of exchange (k_{exch})^a calculated for protons H-3, H-5 and H-9 in EXSY spectra of **1** recorded at 268–308 K

Temperature (K)	268	278	288	298	308
H-3 ^b (δ_H 4.38 \leftrightarrow 4.61 ppm)	0.50	2.14	8.71	19.1	71.1
H-5 ^b (δ_H 4.26 \leftrightarrow 4.50 ppm)	0.47	2.16	8.72	19.5	78.1
H-9 ^b (δ_H 2.53 \leftrightarrow 2.67 ppm)	0.57	2.04	8.45	24.6	59.4

^a Rates of exchange which are quoted are an average of values which were calculated from 3–4 individual EXSY experiments with different mixing times (t_m) recorded at the same temperature—see Experimental.

^b Rate of exchange in s⁻¹.

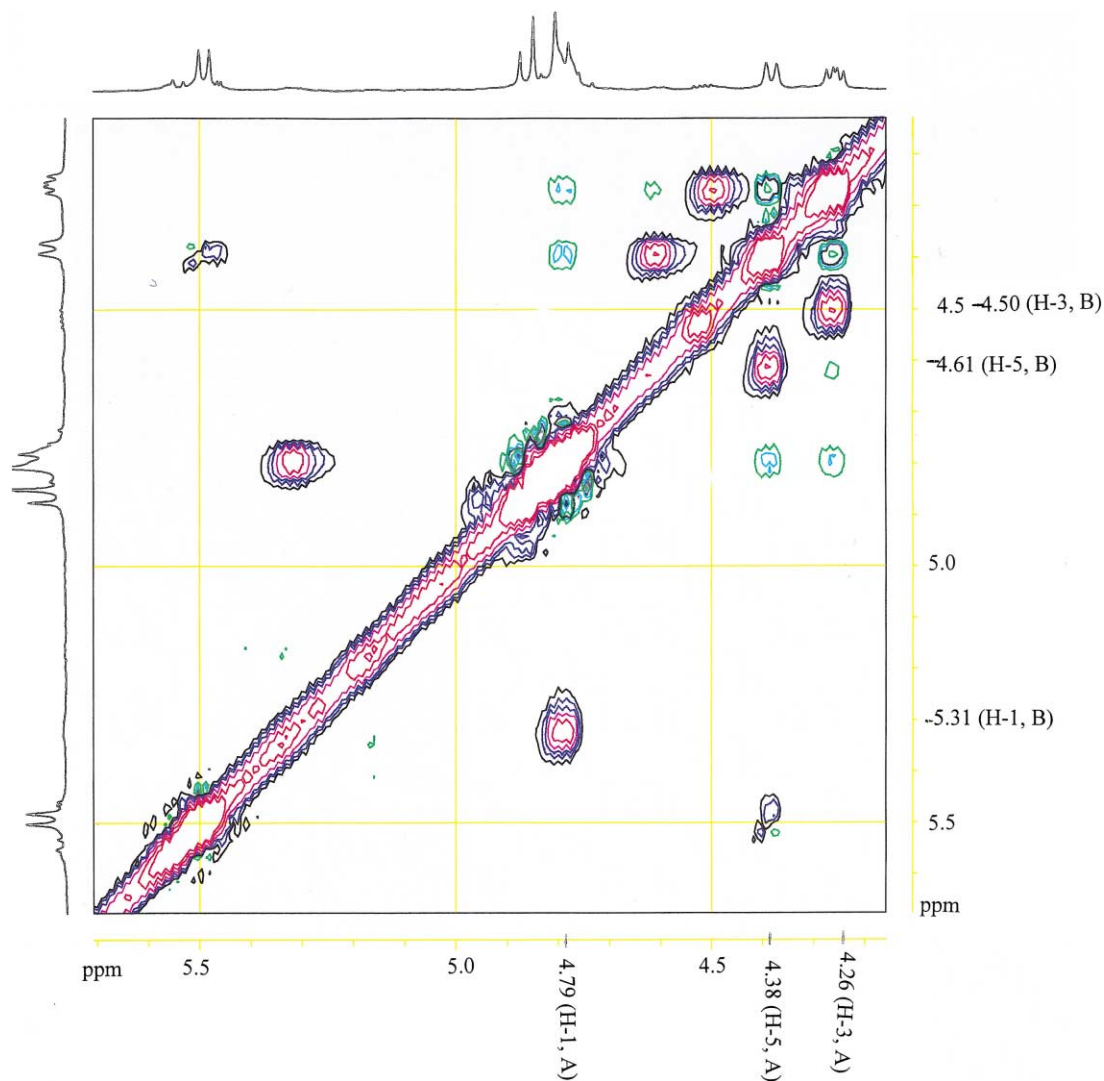


Fig. 3. Expansion of the alkene region of the NOESY spectrum of **1**. Positive cross-peaks due to chemical exchange ("EXSY" peaks) appear as dark blue and red contours and are labeled by the number of the proton undergoing exchange, while negative cross-peaks indicating nuclear Overhauser enhancements appear as light blue and green contours.

conformer B would be expected to result in steric interactions with other atoms around the ten-membered ring, and this effect is presumably the main cause of the higher energy calculated for conformer B (the ring-hydroxyl is equatorial in conformer A and such energetically unfavourable axial-axial interactions are therefore avoided).

Returning to the analysis of nuclear Overhauser enhancements (NOE's) in the NOESY spectrum of **1**, it was apparent that most of the negative cross-peaks seen in the NOESY spectrum of **1** were also consistent with the structure of the lower energy conformer (A), which was predicted by molecular modeling. For example, in the expansion of the alkene region of the NOESY spectrum of **1** shown in Fig. 3, negative cross-peaks (appearing as light blue/green contours) are apparent between all of the resonances for H-3, H-5 and H-1 of conformer A (δ_{H} 4.26, 4.38 and 4.79 ppm, respectively). These and other critical correlations representing NOE's which

were used in confirming the structure of conformer A are indicated by arrows in Fig. 5. Note that positive correlations (dark blue/red contours) are also evident in Fig. 3. These cross-peaks are due to exchange between conformers A and B (H-3, H-5 and H-1 of conformer A occur at δ_{H} 4.26, 4.38 and 4.79 ppm, respectively; while H-3, H-5 and H-1 of conformer B are at δ_{H} 4.50, 4.61 and 5.31 ppm, respectively), as has been discussed above. They are undesired in the context of attempts to interpret NOE's in order to determine spatial relationships within a conformer—their relatively intense appearance in Fig. 3 is due to the long mixing times which were used in order to allow NOE's between protons to develop (t_{m} = 600 ms; as compared with much shorter mixing times which were sufficient to study the exchange phenomenon at ambient temperature—see Experimental). Closer inspection of Fig. 3 also reveals a weak negative cross-peak which would seem to indicate an NOE between H-3 of

conformer A (δ_{H} 4.26 ppm) and H-5 of conformer B (δ_{H} 4.61 ppm).² Since it should not be possible to observe NOE's between protons in two different molecules, this, and other weak negative cross-peaks seen in the NOESY spectrum of compound **1**, must be associated with population transfers due to *both* exchange processes and dipole–dipole interactions, which are occurring simultaneously in solution. This additional layer of complexity encountered when attempting to interpret NOE correlations in the presence of exchange has led us to undertake a further investigation of another germacranolide, parthenolide (**5**), which is commercially available and for which no mention was made of the occurrence of exchange phenomena, when a full assignment of the ^1H resonances was reported by Jacobsson et al. (1995). It was anticipated that analysis of the NOESY spectra of **5** would be simplified as a result of the absence of exchange, and it would then prove possible to obtain independent evidence to support the deductions concerning the lowest energy conformer of the ten-membered ring in compounds **1–4**.

The published X-ray structure for parthenolide (Quick and Rogers, 1976) indicated the same conformation for the ten-membered ring as that which was predicted for the lower energy conformer of the germacranolide ring in **1**, by molecular modeling (Fig. 5), and which appeared to have been confirmed experimentally by the more intense negative cross-peaks seen in the NOESY spectrum of **1**. After fully assigning the ^{13}C and ^1H resonances of parthenolide by 2D-NMR spectroscopic analyses as previously (full ^{13}C NMR assignments for **5** appear in Table 1 for the first time), it was confirmed that the solution conformation of parthenolide is the same as that reported for the solid state. Analysis of the NOESY spectrum of **5** was a relatively straightforward matter, as only negative cross-peaks due to nuclear Overhauser enhancements between protons were observed (critical correlations are indicated by arrows in Fig. 6 and are similar to those used in defining the structure of conformer A of **1** in Fig. 5). The absence of any positive cross-peaks in the NOESY spectrum of parthenolide confirmed that compound **5** is not undergoing any appreciable chemical exchange at room temperature. This is probably due to the replacement of the $\Delta^{4,5}$ double bond in **1–4** by an epoxide group in **5**, which is too bulky to allow the ten-membered ring to easily flip into the alternative but probably much higher energy conformation B (in which this

functional group would be constrained to project *inside* the ring system). The definitive solution conformation found for the ten-membered ring in **5**, therefore, supports the conclusions concerning both the structure of the lower energy conformation of the germacranolide ring-system in compounds **1–4** and the existence of an alternative higher energy conformer for the medium-sized ring present in all these compounds.

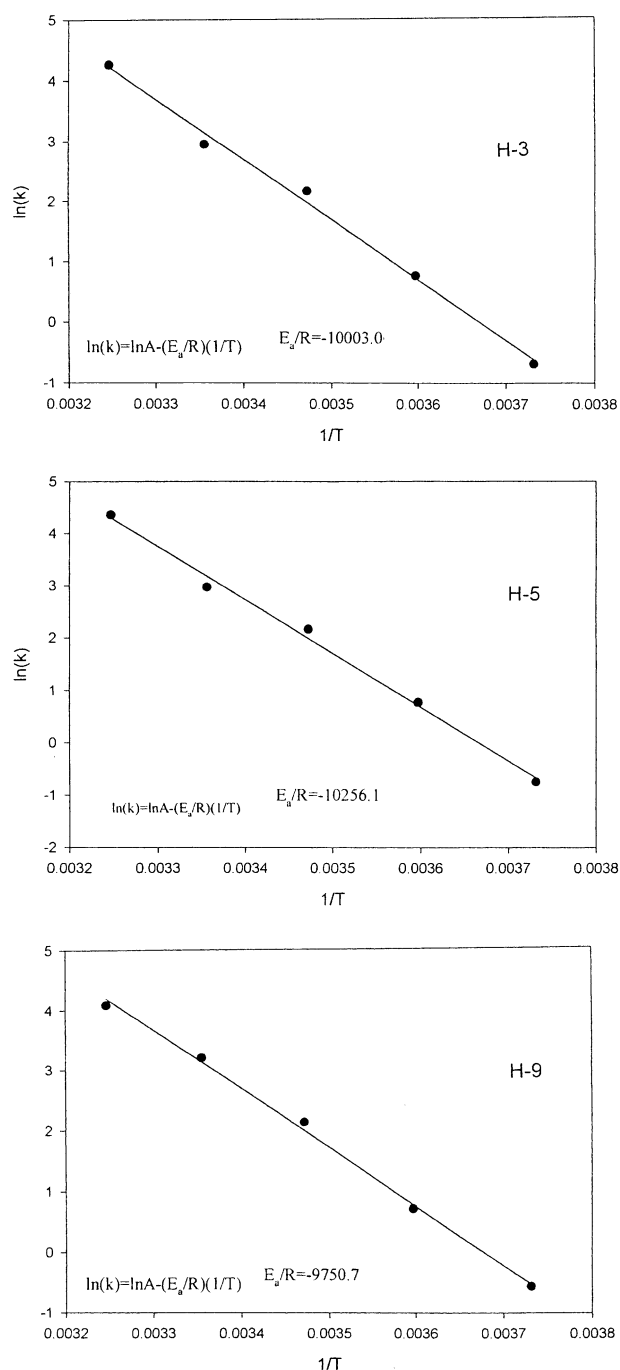


Fig. 4. Arrhenius plots of $\ln k_{\text{exch}}$ against $1/T$ used in estimating the activation barrier to exchange (E_a) for different positions around the ten-membered ring of **1**. Linear regression analysis yielded E_a values of 83.1, 85.3 and 81.1 kJ mol^{-1} for each of H-3, H-5 and H-9, respectively.

² A third type of cross-peak, containing both negative and positive lobes, is also seen in Fig. 3 between H-6 (δ_{H} 5.49 ppm) and H-5 (δ_{H} 4.38 ppm) of conformer A. Such cross-peaks are indicative of strong J -coupling ($^3J_{\text{H-5,H-6}} = 10.1 \text{ Hz}$) and have been ignored in this analysis, as they only reflect information relating to the planar structure of the molecule, which is already provided by ^1H – ^1H COSY experiments.

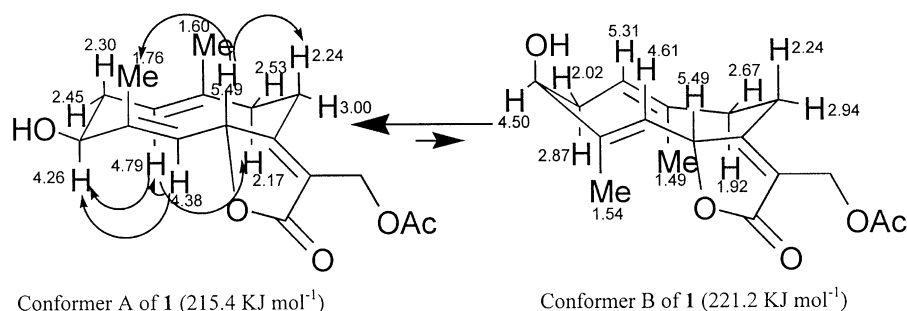


Fig. 5. Two possible conformations for the ten-membered ring in **1**, which were predicted by the results of molecular modeling. Critical nuclear Overhauser enhancements between protons, which confirmed experimentally that **1** existed predominantly as conformer A, are indicated by arrows. Chemical shifts of protons in conformer B, which were deduced from chemical shifts of “EXSY-type” correlations seen from some of the ring protons of conformer A, are indicated on the structure.

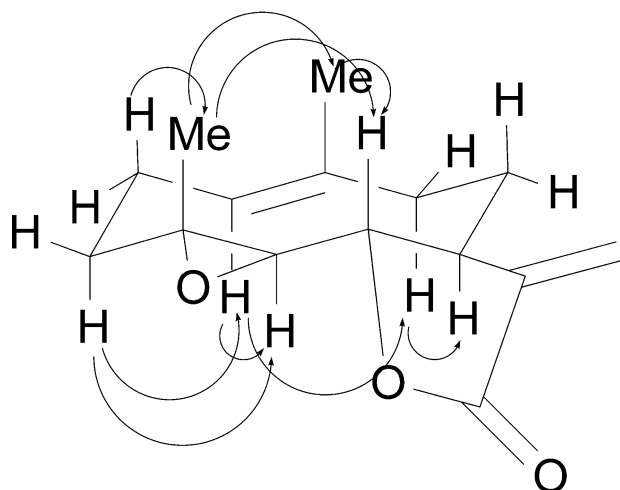


Fig. 6. Solution conformation of parthenolide (**5**) as determined by NOESY (found to be identical with the crystal structure previously described for **5**). Nuclear Overhauser enhancements between protons are indicated by arrows.

3. Experimental

Chemical shifts are expressed in ppm (δ) relative to TMS as internal standard. All NMR spectroscopic experiments were run on a Bruker DRX 500 instrument. Two-dimensional spectra were recorded with 1024 data points in F_2 and 256 data points in F_1 . A mixing time (t_m) of 600 ms (the null point in T_1 inversion recovery experiments for most resonances of **1–4**) was used for recording the NOESY spectra which were used in the analysis of nOe's at 298 K. HREIMS were recorded at 70 eV on a Finnigan-MAT 95 MS spectrometer. IR spectra were recorded in CHCl_3 on a Shimadzu FTIR-8201 PC spectrometer. TLC plates were developed using *p*-anisaldehyde. Column chromatography was performed using silica gel 60–200 μm (Merck). HPLC separations were performed using a Varian chromatograph equipped with RI star 9040 and UV 9050 detectors and an Intersil PREP-SIL column (20 mm \times 25 cm), operating isocratically with EtOAc/*n*-hexane mixtures at a flow rate of 8 ml/min.

3.1. Plant material

A. myriantha was collected from Southern Yunnan province, China in August 1999. Taxonomic identification was made by Professor Ling Yeou-Ruenn of the South China Botanical Garden, Guangzhou PRC, and a voucher specimen is kept at the University of Hong Kong Herbarium (D.Q. Zhou s.n., 19 Aug 1999 HKU).

3.2. Extraction and isolation

The aerial parts of *A. myriantha* (650 g) were pulverized to a fine powder under liquid N_2 and repeatedly extracted with CH_2Cl_2 at room temperature. The combined solvent extracts were dried (MgSO_4) and solvent was removed under reduced pressure to yield a dark brown gum (20.5 g; 3.2% w/w) which was subjected to gradient CC (developing solvents 100% *n*-hexane \rightarrow 100% EtOAc \rightarrow 100% MeOH). Fractions from CC were further purified by HPLC yielding: **1** (5.6 mg, R_t 53.1 min in 45% EtOAc/*n*-hexane/1.2% CH_3COOH); **2** (3.3 mg, R_t 18.7 min in 45% EtOAc/*n*-hexane); **3** (2.8 mg, R_t 20.6 min in 45% EtOAc/*n*-hexane); and **4** (5.9 mg, R_t 48.1 min in 30% EtOAc/*n*-hexane).

3.3. 13-Acetoxy-3 β -hydroxy-germacra-1(10)*E*,4*E*,7(11)-trien-12,6 α -olide (**1**)

Gum: $[\alpha]_D +53.0$ (c 0.6, CHCl_3); IR (CHCl_3) ν_{max} 3530 (*br*), 3026, 2932, 1755, 1456, 1369, 1232 cm^{-1} ; For ^1H NMR and ^{13}C NMR data, see Tables 1 and 2 (see also Zdero and Bohlmann (1990) for ^1H NMR and MS).

3.4. Determination of the rate of exchange (k_{exch}) for *H*-3, *H*-5 and *H*-9 in EXSY spectra of **1** over the temperature range 268–308 K

Variable temperature-NOESY (EXSY) spectra, which were acquired in order to measure the rate and activation barrier for conformational exchange of **1** in CDCl_3 solution, were recorded with the probehead of the

NMR spectrometer at the following temperatures³ and with the mixing time (t_m) set to 3 or 4 values (indicated in parentheses) at each temperature: 268 K (t_m = 100, 250 and 500 ms), 278 K (t_m = 20, 50 and 100 ms), 288 K (t_m = 10, 20 and 50 ms), 298 K (t_m = 5, 10, 20 and 50 ms) and 308 K (t_m = 2, 5, 10 and 20 ms). The values of t_m which are shown for a particular temperature⁴ were found to give fairly good reproducibility in the rates of exchange (k_{exch}) which were calculated for H-3, H-5 and H-9 according to the procedure given below, and the average value calculated from the 3 or 4 experiments with different t_m values is quoted in Table 3.

In each spectrum, the rates of proton exchange between conformers A (major) and B (minor) were calculated by measuring volume integrals both for the diagonal peaks (I_{AA} , I_{BB}) and for the off-diagonal peaks (I_{AB} , I_{BA}) for resonances corresponding to each of H-3 (I_{AA} = 4.20–4.30 ppm in F_2 , 4.20–4.30 ppm in F_1 ; I_{BB} = 4.45–4.53 ppm in F_2 , 4.45–4.53 ppm in F_1 ; I_{AB} = 4.20–4.30 ppm in F_2 , 4.45–4.53 ppm in F_1 ; I_{BA} = 4.45–4.53 ppm in F_2 , 4.20–4.30 ppm in F_1); H-5 (I_{AA} = 4.32–4.42 ppm in F_2 , 4.32–4.42 ppm in F_1 ; I_{BB} = 4.55–4.65 ppm in F_2 , 4.55–4.65 ppm in F_1 ; I_{AB} = 4.32–4.42 ppm in F_2 , 4.55–4.65 ppm in F_1 ; I_{BA} = 4.55–4.65 ppm in F_2 , 4.32–4.42 ppm in F_1); and H-9 (I_{AA} = 2.47–2.57 ppm in F_2 , 2.47–2.57 ppm in F_1 ; I_{BB} = 2.62–2.72 ppm in F_2 , 2.62–2.72 ppm in F_1 ; I_{AB} = 2.47–2.57 ppm in F_2 , 2.62–2.72 ppm in F_1 ; I_{BA} = 2.62–2.72 ppm in F_2 , 2.47–2.57 ppm in F_1).

The mole fractions of conformer A (X_A) and of conformer B (X_B) at a given temperature were determined from integration of the peaks for the well-resolved H-5 resonance in 1D ^1H -NMR (δ_{H} 4.38 ppm for conformer A and δ_{H} 4.61 ppm for conformer B). The rate of exchange (k_{exch} , which is the sum of the rates for the forward and back reactions $k_{AB} + k_{BA}$) was then calculated independently for each of H-3, H-5 and H-9 according to the formula:

$$k_{\text{exch}} = 1/t_m(\ln((r + 1)/(r - 1)))$$

³ The optimum rate of exchange for EXSY studies is determined by the T_1 relaxation rate for ^1H and is generally around 10 s⁻¹ (Perrin and Dwyer, 1990); this range of temperatures was chosen such that k_{exch} for the middle member of the series (288 K) was close to this value.

⁴ The ranges of values used for a given temperature are based on the assumption that the optimized mixing time should be set roughly as $t_m \approx 1/(T_1^{-1} + k_{AB} + k_{BA})$ where T_1 is the longitudinal relaxation rate and k_{AB} and k_{BA} are the rates of forward and back reactions, respectively ($k_{\text{exch}} = k_{AB} + k_{BA}$). Within these ranges of t_m , the calculated values for k_{exch} were found to be fairly reproducible ($\pm 10\%$) although, in general, there was a slight decrease in the calculated value of k_{exch} as t_m was increased. At very large values of t_m (not shown), the rate sometimes became undefined (due to the necessity of taking the logarithm of a negative number)—this may be due to relaxation effects dominating at long t_m or to kinetic effects becoming so large as to be insensitive to the rate parameters (Perrin and Dwyer, 1990).

where, $r = 4X_AX_B(I_{AA} + I_{AB})/(I_{AB} + I_{BA}) - (X_A - X_B)^2$

3.5. Determination of the activation barrier (E_a) to exchange for H-3, H-5 and H-9 in EXSY spectra of **1**

The activation energy to exchange (E_a) for each of H-3, H-5 and H-9 was calculated by plotting the natural logarithm of k_{exch} for each proton against the reciprocal of the absolute temperature ($1/T$) for each of the five temperatures studied in the previous section, and then performing a linear regression on the resulting data (using the programme Sigmaplot) according to the equation:

$$\ln k_{\text{exch}} = \ln A - (E_a/RT)$$

where, $R = 8.31451 \text{ JK}^{-1} \text{ mol}^{-1}$ (the gas constant) and $A \text{ (s}^{-1}\text{)}$ is a probability factor.

r^2 Values for the linear-regression fit to the data-points shown in Fig. 4 were uniformly greater than 0.99, indicating a high level of confidence in the values of E_a obtained.

3.6. Experimentally-determined energy difference (ΔE) between conformers A and B of **1**

The difference in energy (ΔE) between the two conformers A and B at ambient temperature for the NMR probehead (298 K) was calculated according to the equation:

$$[N]_B/[N]_A = \exp(-\Delta E/RT)$$

where, $[N]_B$ is the number of molecules in conformer B; and $[N]_A$ is the number of molecules in conformer A

$[N]_A$ and $[N]_B$ were estimated from integration of the peaks for the well-resolved H-5 resonance in 1D ^1H -NMR (δ_{H} 4.38 ppm for conformer A and δ_{H} 4.61 ppm for conformer B) as being in a ratio of 100:15.7, which implies an energy difference between conformers A and B of 4.58 kJ mol⁻¹.

3.7. 13-Acetoxy 3 β -tigloyl-germacra-1(10)*E*,4*E*,7(11)-trien-12,6 α -olide (**2**)

Gum: $[\alpha]_D + 112.7$ (c 0.3, CHCl_3); IR (CHCl_3) ν_{max} 3028, 2932, 2856, 1759, 1717, 1259 cm⁻¹; ^1H NMR and ^{13}C NMR, see Tables 1 and 2; HREIMS: m/z (rel. int.) 388.1885 (15) (calc. for $\text{C}_{22}\text{H}_{28}\text{O}_6$, 388.1886), 360 (10), 321 (20), 307 (25), 260 (15), 246 (55), 228 (70), 213 (45), 149 (100).

3.8. 13-Acetoxy-3 β -propanoyl-germacra-1(10)*E*,4*E*,7(11)-trien-12,6 α -olide (**3**)

Gum: $[\alpha]_D + 97.9$ (c 0.3, CHCl_3); IR (CHCl_3) ν_{max} 3026, 2986, 1757, 1462, 1367, 1229 cm⁻¹; ^1H NMR and

^{13}C NMR, see Tables 1 and 2; HREIMS: m/z (rel. int.) 362.1728 (5) (calc. for $\text{C}_{20}\text{H}_{26}\text{O}_6$, 362.1729), 246 (100), 228 (35), 213 (20), 178 (95), 149 (30).

3.9. 13-Acetoxy-3 β -(3-methylbutanoyl)-germacra-1(10)*E*,4*E*,7(11)-trien-12,6 α -olide (**4**)

Gum: $[\alpha]_{\text{D}} + 25.6$ (c 0.6, CHCl_3); IR (CHCl_3) ν_{max} 2963, 2930, 1759, 1458, 1369, 1332 cm^{-1} ; ^1H NMR and ^{13}C NMR, see Tables 1 and 2; HREIMS: m/z (rel. int.) 390.2040 (5) (calc. for $\text{C}_{22}\text{H}_{30}\text{O}_6$, 390.2042), 260 (20), 246 (50), 228 (20), 178 (35), 149 (35), 85 (100).

3.10. Parthenolide (4,5-epoxy-germacra-1(10)*E*, 11(13)-dien-12,6 α -olide) (**5**)

Parthenolide was purchased from the Aldrich chemical company (Cat. No. 38,428-3).

Acknowledgements

We are grateful to Mr. Dequn Zhou for collecting the plant material and Professor Ling Yeou-Ruenn for taxonomic identification of *A. myriantha*. The Chemistry Department of The University of Hong Kong provided a postgraduate studentship to Mr. H.-F. Wong. This work was supported by a grant from the Committee on Research and Conference Grants.

References

- Adekenov, S.M., 2000a. *Artemisia glabella* Kar et Kir: a source of the new antitumor preparation "Arglabin". *Phytomedicine* Jena 7, 103.
- Adekenov, S. M., 2000b. Arglabin compounds and therapeutic uses thereof. Official Gazette of the United States Patent and Trademark Office Patents, June 2000.
- Appendino, G., Gariboldi, P., Menichini, F., 1991. The stereochemistry of arglabin, a cytotoxic guaianolide from *Artemisia myriantha*. *Fitoterapia* 62, 275–276.
- Atkins, P.W., 1999. *Physical Chemistry*, 6th Edition. Oxford University Press, Oxford, pp. 775–777.
- Braun, S., Kalinowski, H.-O., Berger, S., 1996. 100 and more basic NMR experiments. VCH, Weinheim, pp. 341–343.
- Evans, J.N.S., 1995. *Biomolecular NMR Spectroscopy*. Oxford University Press, Oxford, pp. 43–50.
- Jacobsson, U., Kumar, V., Saminathan, S., 1995. Sesquiterpene lactones from *Michelia champaca*. *Phytochemistry* 39, 839–843.
- Jakupovic, J., Kleymer, H., Bohlmann, F., Graven, E.H., 1988. Glaucolides and guaianolides from *Artemisia afra*. *Phytochemistry* 27, 1129–1133.
- Jakupovic, J., Tan, R.X., Bohlmann, F., Boldt, P.E., Jia, Z.J., 1991. Sesquiterpene lactones from *Artemisia ludoviciana*. *Phytochemistry* 30, 1573–1577.
- Ling, Y.-R., 1986. *Wuyi Science Journal* 6, 351.
- Mohamadi, F., Richards, N.G.J., Guida, W.C., Liskamp, R., Lipton, M., Caufield, C., Chang, G., Hendrickson, T., Still, W.C., 1990. MacroModel—an integrated software system for modeling organic and bioorganic molecules using molecular mechanics. *J. Comput. Chem.* 11, 440–467.
- Perrin, C.L., Dwyer, T.J., 1990. Application of two-dimensional NMR to kinetics of chemical exchange. *Chemical Reviews* 90, 935–967.
- Quick, A., Rogers, D., 1976. Crystal and molecular structure of parthenolide [4,5-epoxygermacra-1(10), 11(13)-dien-12,6-olactone]. *J. Chem. Soc., Perkin Trans. II*, 465–469.
- Zdero, C., Bohlmann, F., 1990. Glaucolides, fulvenoglucolides and other sesquiterpene lactones from *Pentzia* species. *Phytochemistry* 29, 189–194.